Analysis of Metal Flow under Extrusion and Sheet Rolling by the Finite Element Method

Chaiyarit Oupichit
Graduate Student

Pramote Dechaumphai
Professor

Department of Mechanical Engineering, Faculty of Engineering,
Chulalongkorn University, Bangkok 10330

Abstract

This paper presents a finite element computational method for two-dimensional non-Newtonian metal flow under extrusion. The thermal effect from metal deformation and internal heat flow is coupled in the system. Finite element equations corresponding to the problem were derived from the related governing differential equations using the Galerkin weighted residuals method. The derived finite element equations were then used in the development of a computer program that can be executed on standard personal computers. The program was verified by comparing the computational solutions with those obtained from the metal deformation analysis theory and the experimental data. More realistic extrusion problems were then solved using the developed program for predicting detailed flow behavior. The program was also used for the analysis of sheet metal rolling problems. Results were verified with solutions from theory of sheet rolling as well as experimental data. The adaptive remeshing technique was also applied to further improve the analysis solution accuracy.

1. Introduction

In most of metal forming processes, the external force is applied to the metal for changing its original shape to a final product. The metal deformation passes from elastic through plastic with large strain behavior. The solid is incapable to support deviatoric stress without motion. As a result, it behaves similarly to a fluid. If the elastic strains are negligible compared to the large plastic strain, the solid deformation may be treated as non-Newtonian viscous incompressible fluid flow. The analogy is commonly know as the "flow formulation" [1] which is a valuable technique for investigating metal forming behavior.

Temperature is an important parameter of metal forming. When the metal is deformed, the inside temperature changes either due to an external imposition of heat, or due to the spontaneous heat generation following the energy dissipation of the process. Most of metal forming materials are sensitive to the temperature change. Another word, the yield stress of materials varies with the temperature. Thus the deforming process is significantly related to the thermal coupling. The metal flow with thermal coupling is governed by a set of partial differential equations which are the conservation of mass, momentums, and energy.

This paper studies two-dimensional metal flow behavior by using the finite element method (FEM). The method of weighted residuals, together with Galekin approach, is used to derive the corresponding finite element equations [2]. The six-node quadratic triangular element is selected in the study. A computer program is also developed from the derived finite element equations.

Applications of the two-dimensional metal flow presented in this paper are the extrusion of metal billet pass through square die and the sheet metal rolling. Both applications have the same objective in order to reduce the thickness of original shape. For extrusion, the adequate extrusion force is an important value needed by design engineer. This unknown is computed from the developed program as well as the velocity components, pressure and temperature distributions. The sheet rolling application has similar deformation behavior as the extrusion except the nature of boundary conditions. The roll force and roll torque are the two desired values of the problem.

The predicted finite element solutions are compared with the analytical solution as well as the experimental data. An adaptive remeshing is also applied to improve the solution accuracy, to minimize the required memory of computer and to reduce the computational time.

2. Theoretical Formulation

2.1. Governing differential equations

The governing differential equations for predicting the non-Newtonian viscous incompressible metal flow behavior are the conservation of mass, momentum and energy equations. For low speed steady-state flow, these differential equations are [3],

conservation of momentums,

$$\frac{\partial \sigma_x}{\partial x} + \frac{\partial \tau_{yx}}{\partial y} = 0 \tag{1a}$$

$$\frac{\partial \tau_{xy}}{\partial x} + \frac{\partial \sigma_y}{\partial y} = 0 \tag{1b}$$

conservation of mass,

$$\frac{\partial u}{\partial x} + \frac{\partial v}{\partial y} = 0 \tag{2}$$

conservation of energy,

$$\rho c\left(u\frac{\partial T}{\partial x} + v\frac{\partial T}{\partial y}\right) = \frac{\mu(\dot{\bar{\varepsilon}})^2}{J} + k\frac{\partial^2 T}{\partial x^2} + k\frac{\partial^2 T}{\partial y^2} \tag{3}$$

The stress components are,

$$\sigma_x = -p + 2\mu\frac{\partial u}{\partial x} \tag{4a}$$

$$\sigma_y = -p + 2\mu\frac{\partial v}{\partial y} \tag{4b}$$

$$\tau_{xy} = \tau_{yx} = \mu\left(\frac{\partial u}{\partial y} + \frac{\partial v}{\partial x}\right) \tag{4c}$$

where u and v are velocity components in x and y directions respectively, p is pressure, ρ is fluid density, μ is viscosity coefficient, k is thermal conductivity, c is specific heat, T is temperature, $\dot{\bar{\varepsilon}}$ is effective strain rate and J is mechanical-heat equivalent value.

For ideal plastic metal flow, the viscosity is in the form [4],

$$\mu = \frac{\sigma_Y(T)}{\sqrt{3}\dot{\bar{\varepsilon}}} \tag{5}$$

where σ_Y is the temperature dependent yield and $\dot{\bar{\varepsilon}}$ is effective strain rate given by [5],

$$\dot{\bar{\varepsilon}} = \sqrt{2\dot{\varepsilon}_{ij}\dot{\varepsilon}_{ij}} \tag{6}$$

where $\dot{\varepsilon}_{ij}$ is strain rate component.

Appropriate boundary conditions of metal forming problems normally consist of specifying velocity components as well as heat fluxes along the edges,

$$\begin{aligned} u &= u_1(x,y) \\ v &= v_1(x,y) \\ q &= q_1(x,y) \end{aligned} \tag{7}$$

2.2 The Finite Element Formulation

The six-node quadratic triangular element suggested in Ref. [6] is selected to derive the finite element equations. The element interpolation functions are,

$$u(x,y) = \lfloor N \rfloor \{u\} \tag{8a}$$

$$v(x,y) = \lfloor N \rfloor \{v\} \tag{8b}$$

$$T(x,y) = \lfloor N \rfloor \{T\} \tag{8c}$$

$$p(x,y) = \lfloor H \rfloor \{p\} \tag{8d}$$

where $\lfloor N \rfloor$ is quadratic interpolation function matrix and $\lfloor H \rfloor$ is linear interpolation function matrix.

The method of weighted residuals with Galerkin approach [2] is then applied to the differential equations, Eqs. (1-3),

$$\int_A N_i\left(\frac{\partial \sigma_x}{\partial x} + \frac{\partial \tau_{xy}}{\partial y}\right)dA = 0 \tag{9a}$$

$$\int_A N_i\left(\frac{\partial \tau_{xy}}{\partial x} + \frac{\partial \sigma_y}{\partial y}\right)dA = 0 \tag{9b}$$

$$\int_A H_i\left(\frac{\partial u}{\partial x} + \frac{\partial v}{\partial y}\right)dA = 0 \tag{10}$$

$$\int_A N_i\left(k\frac{\partial^2 T}{\partial x^2} + k\frac{\partial^2 T}{\partial y^2} + \frac{\mu\dot{\bar{\varepsilon}}^2}{J} - \mu\frac{\partial T}{\partial x} - v\frac{\partial T}{\partial y}\right)dA = 0 \tag{11}$$

where A is the element area. Gauss's theorem is applied to generate the boundary integral terms associated with the surface tractions to yield,

$$\int_{S_o} N_i(\sigma_x l + \tau_{xy} m)dS_o = \int_A \left(\frac{\partial N_i}{\partial x}\sigma_x + \frac{\partial N_i}{\partial y}\tau_{xy}\right)dA \tag{12a}$$

$$\int_{S_o} N_i(\tau_{xy} l + \sigma_y m)dS_o = \int_A \left(\frac{\partial N_i}{\partial x}\tau_{xy} + \frac{\partial N_i}{\partial y}\sigma_y\right)dA \tag{12b}$$

$$\begin{aligned} &\rho c\int_A N_i\left(u\frac{\partial T}{\partial x} + v\frac{\partial T}{\partial y}\right)dA + k\int_A \frac{\partial N_i}{\partial x}\frac{\partial T}{\partial x}dA \\ &+ k\int_A \frac{\partial N_i}{\partial y}\frac{\partial T}{\partial y}dA = k\int_{S_w} N_i\left(\frac{\partial T}{\partial x}l + \frac{\partial T}{\partial y}m\right)dS_w \\ &+ \int_A N_i\left(\frac{\mu\dot{\bar{\varepsilon}}^2}{J}\right)dA \end{aligned} \tag{13}$$

In the above equations, S_o and S_w are the element boundary associated with the mechanical and thermal load, respectively. By substituting Eq. (4) into Eq. (12), the above set of equations becomes,

$$\int_A \left[\left(2\mu \frac{\partial u}{\partial x} - p \right) \frac{\partial N_i}{\partial x} + \mu \left(\frac{\partial u}{\partial y} + \frac{\partial v}{\partial x} \right) \frac{\partial N_i}{\partial y} \right] dA = \int_{S_o} N_i P_x dS_o \quad (14a)$$

$$\int_A \left[\mu \left(\frac{\partial u}{\partial y} + \frac{\partial v}{\partial x} \right) \frac{\partial N_i}{\partial x} + \left(2\mu \frac{\partial v}{\partial y} - p \right) \frac{\partial N_i}{\partial y} \right] dA = \int_{S_o} N_i P_y dS_o \quad (14b)$$

$$\int_A H_i \left(\frac{\partial u}{\partial x} + \frac{\partial v}{\partial y} \right) dA = 0 \quad (15)$$

$$\int_A N_i \left(u \frac{\partial T}{\partial x} + v \frac{\partial T}{\partial y} \right) dA + \frac{k}{\rho c} \int_A \frac{\partial N_i}{\partial x} \frac{\partial T}{\partial x} dA + \frac{k}{\rho c} \int_A \frac{\partial N_i}{\partial y} \frac{\partial T}{\partial y} dA = \frac{1}{\rho c} \int_{s_w} N_i q_w dS_w + \frac{1}{\rho c} \int_A N_i \left(\frac{\mu \dot{\bar{\varepsilon}}^2}{J} \right) dA \quad (16)$$

Applying the element interpolation functions for velocity, pressure and temperature from Eq. (8), the above equations can be written in matrix form as,

$$2\mu [M_{xx}]\{u\} + \mu [M_{yy}]\{u\} + \mu [M_{xy}]\{v\} - [H_x]\{p\} = \{R_u\} \quad (17a)$$

$$\mu [M_{yx}]\{u\} + \mu [M_{xx}]\{v\} + 2\mu [M_{yy}]\{v\} - [H_y]\{p\} = \{R_v\} \quad (17b)$$

$$[H_x]^T \{u\} + [H_y]^T \{v\} = \{0\} \quad (18)$$

$$u[K_x]\{T\} + v[K_y]\{T\} + \frac{k}{\rho c}[M_{xx}]\{T\} + \frac{k}{\rho c}[M_{yy}]\{T\} = \{D\} + \{Q\} \quad (19)$$

where

$$[M_{xx}] = \int_A \left\{ \frac{\partial N}{\partial x} \right\} \left[\frac{\partial N}{\partial x} \right] dA \quad (20a)$$

$$[M_{yy}] = \int_A \left\{ \frac{\partial N}{\partial y} \right\} \left[\frac{\partial N}{\partial y} \right] dA \quad (20b)$$

$$[M_{xy}] = [M_{yx}]^T = \int_A \left\{ \frac{\partial N}{\partial y} \right\} \left[\frac{\partial N}{\partial x} \right] dA \quad (20c)$$

$$[H_x] = \int_A \left\{ \frac{\partial N}{\partial x} \right\} [H] dA \quad (20d)$$

$$[H_y] = \int_A \left\{ \frac{\partial N}{\partial y} \right\} [H] dA \quad (20e)$$

$$[K_x] = \int_A \{N\} \left[\frac{\partial N}{\partial x} \right] dA \quad (20f)$$

$$[K_y] = \int_A \{N\} \left[\frac{\partial N}{\partial y} \right] dA \quad (20g)$$

$$[K_y] = \int_A \{N\} \left[\frac{\partial N}{\partial y} \right] dA \quad (20h)$$

$$\{R_v\} = \int_{S_o} \{N\} P_y dS_o \quad (20i)$$

$$\{D\} = \frac{1}{\rho c} \int_{S_w} \{N\} q_w dS_w \quad (20j)$$

$$\{Q\} = \frac{\mu \dot{\bar{\varepsilon}}^2}{\rho c J} \int_A \{N\} dA \quad (20k)$$

These finite element equations were used in the development of a computer program. The program was then evaluated by examples of metal extrusion that are presented in following section.

3. Examples of Metal Extrusion

3.1 Square Die Extrusion

The 50% reduction of square die extrusion problem is used to evaluate the finite element method by comparing the results with those obtained from the Slip-line theory. The metal is assumed to be copper. The contact condition is assumed frictionless and die is rigid. The dimensions with boundary conditions of problem are shown in Fig. 1.

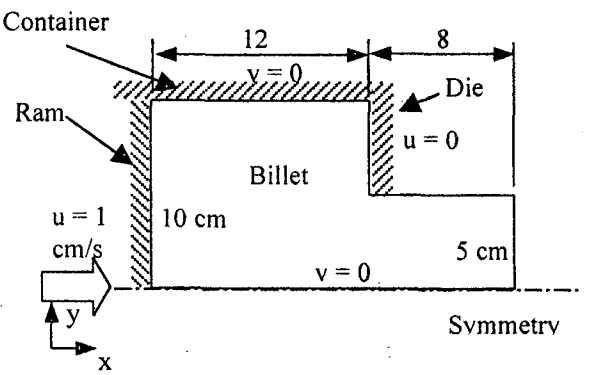

Fig. 1 - The 50% reduction of square die forward extrusion problem.

From the Slip-line theory [7], the extrusion pressure, P, is,

$$\frac{P}{2\tau_{yield}} = 1.3 \quad (23)$$

where τ_{yield} is shear yield stress of the copper which is 1,000 kg/cm^2. Thus the extrusion pressure is 2,600 kg/cm^2.

Figure 2 shows a finite element model consisting of 2,337 nodes and 1,112 elements. Because of the symmetry of the problem, only half model is used in the computation. The predicted velocity and pressure distributions are shown in Fig. 3. The predicted pressure on ram is 2664.3 kg/cm^2 which is 2.5% different from Slip-line solution.

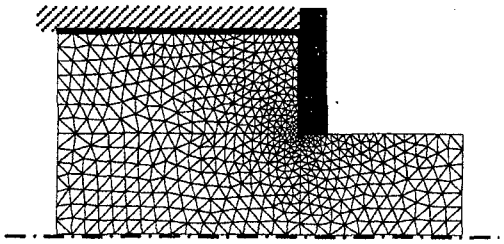

Fig. 2 - Finite element model for square die extrusion problem.

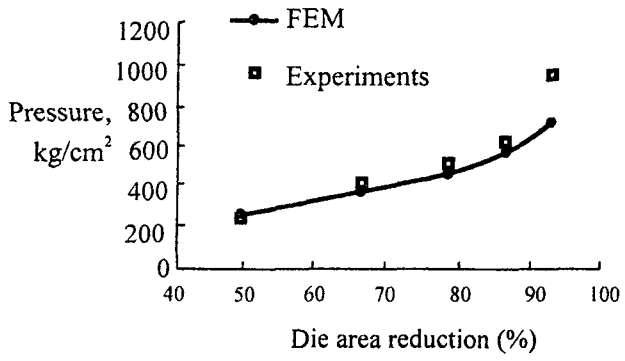

Fig. 4 - Comparison of extrusion pressures between the experimental data and finite element solution for different die area reductions.

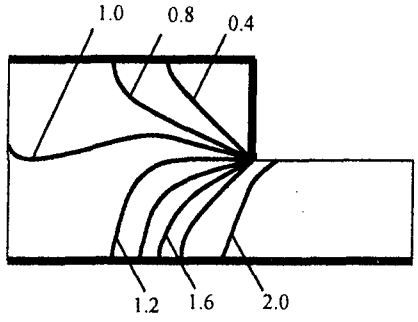

(a) Predicted velocity contours (cm/s).

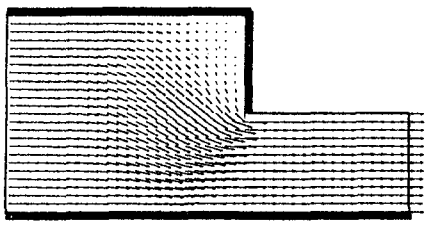

(b) Predicted velocity vectors.

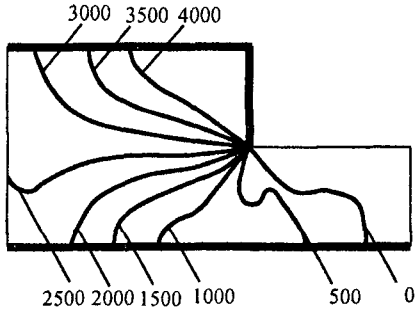

(c) Predicted pressure contours (kg/cm^2).

Fig. 3 - Finite element solution for square die extrusion problems.

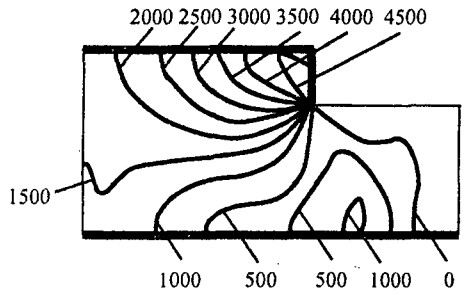

(a) 30% die area reduction.

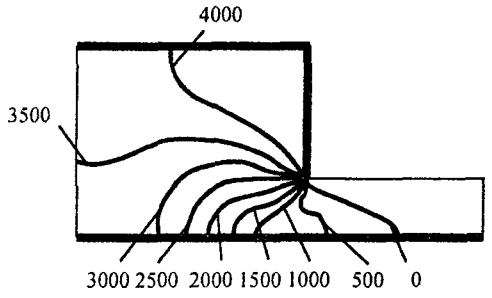

(b) 70% die area reduction.

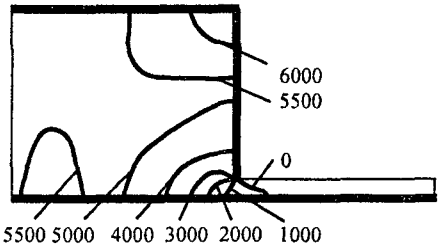

(c) 90% die area reduction.

Fig. 5 - Predicted pressure contours (kg/cm^2) of different die area reductions.

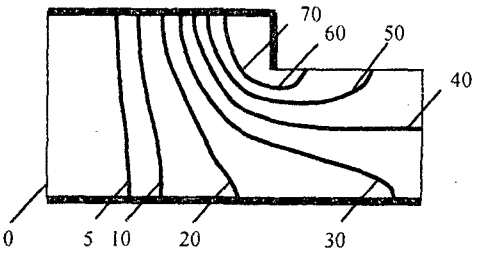

(a) 30% die area reduction.

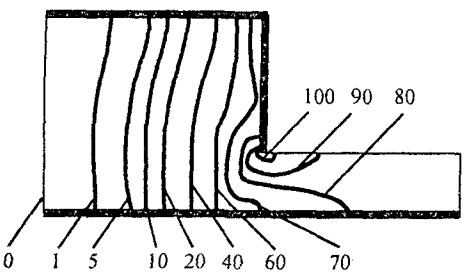

(b) 70% die area reduction.

Fig. 6 - Predicted risen temperature (°C) in different die area reduction.

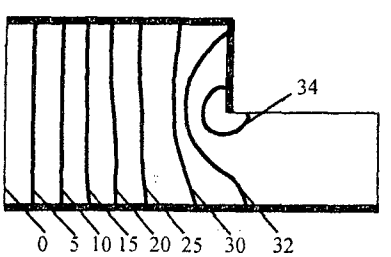

(a) Ram velocity 0.1 cm/s.

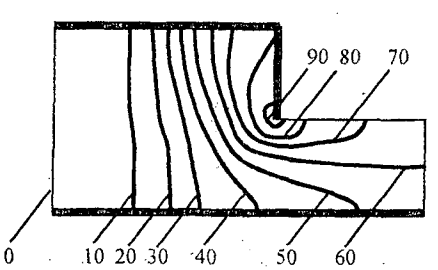

(b) Ram velocity 1 cm/s.

Fig. 7 - Predicted risen temperature (°C) in different extrusion speed.

3.2 Effect of die area reduction and extrusion speed to the temperature distribution

A series of experiments for extrusion pressures in steady-state symmetric forward extrusion has been performed by W. Johnson [8] using pure lead with well lubricated condition. The experimental solutions are compared with the finite element solutions in various die area reduction. Good agreements are obtained as shown in Fig. 4.

The predicted pressure distribution for different die area reductions are shown in Fig. 5. The effect of the die area reduction and the extrusion speed to the increased temperature are illustrated in Figs. 6 and 7, respectively.

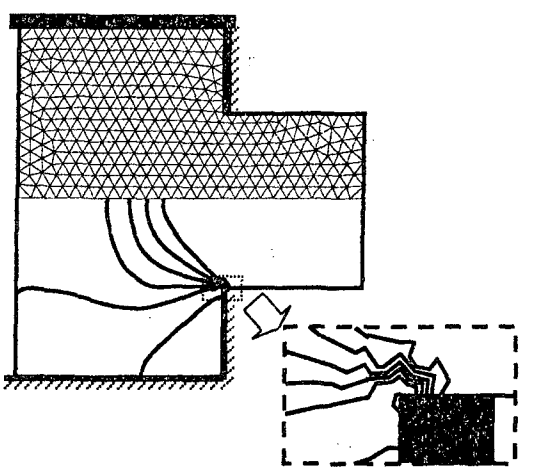

(a) Before remeshing.

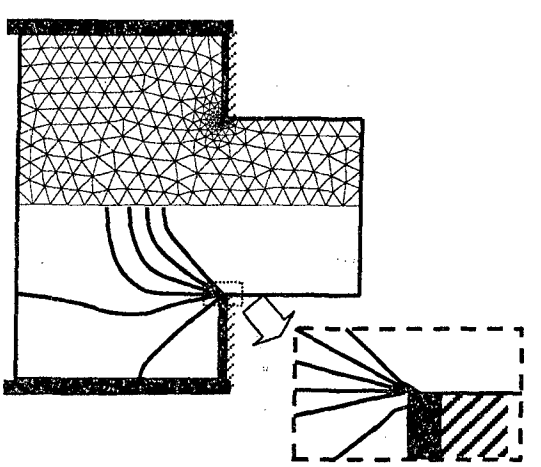

(b) After remeshing.

Fig. 8 - Finite element models and the predicted velocity contours for both before and after applying the adaptive remeshing technique.

3.3 Adaptive remeshing

The predicted finite element solution of the velocity and pressure distributions can be improved by applying the adaptive remeshing technique [9]. The technique places small elements in the regions of large solution gradients automatically to increase the solution accuracy. At the same time, larger elements are placed in the other regions to reduce the total number of unknowns and the computational time. Figs. (8a) and (8b) show the finite element models and the corresponding velocity contours of both before and after applying the adaptive remeshing technique, respectively.

4. Sheet Rolling

Sheet rolling is one of the important processes in metal forming. Sheet metal is squeezed in its transverse direction by plastically deformed passing between rolls for reducing its thickness. The behavior of plastic deformation is obtained by solving the set of governing differential equations as shown in Eqs. (1-3). The theory of rolling aims at relating the external forces, such as roll force and roll torque [10], to the mechanical strength properties of rolled material. The developed program has been used to calculate these external forces, as well as the contours of velocity components, pressures and temperatures through its thickness. The calculation was performed under plane strain condition. Sheet metal was rigid-ideal plastic material and the rolls were perfectly rigid. Non-slip condition was assumed to the contact surface between rolls and sheet metal.

Alexander and Ford [11] presented the empirical formulations for calculating the roll force and roll torque under the plane strain, rigid-ideal plastic and temperature independent material, rigid rolls and non-slip condition. Their solutions are compared with the finite element method. The model of sheet rolling is shown in Fig. 9. The velocity and pressure distribution are shown in Fig. 10. The roll force and torque are obtained from the calculation of forces along the contact surface. The comparing results are shown in table 1.

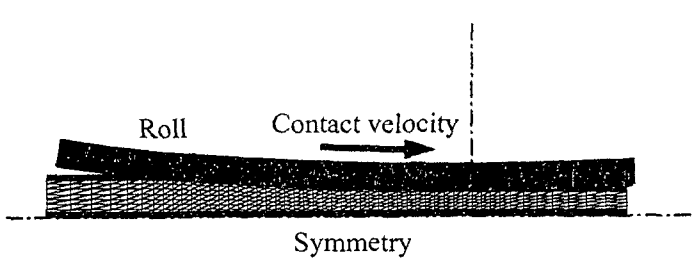

Fig. 9 - Finite element model of sheet rolling.

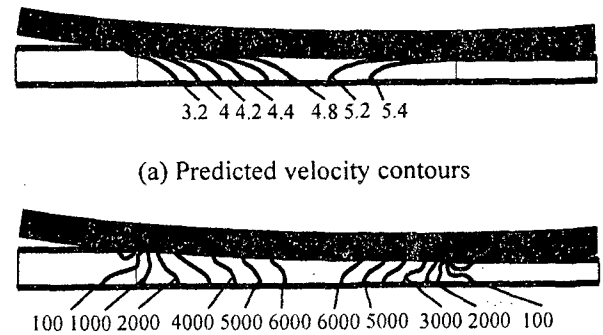

(a) Predicted velocity contours

(b) Predicted pressure contours

Fig. 10 - Finite element solution of rolling problem

Table 1 Comparative results between finite element solution, and analytical solution [11] for sheet metal rolling

	Finite Element	Alexander & Ford [11]	Difference (%)
Roll Force (kg/cm)	9540	9160	4.2
Roll Torque (kg.cm/cm)	19880	19050	4.4

Sim's experimental solutions [12] have also been used to confirm the finite element formulation. Pure lead was chosen as the experimental material. The roll force and roll torque were measured in different roll reduction. The comparison with finite element solutions is shown in Fig. 11. Figure 12 also shows the effect of the contact velocity to the temperature increment for sheet rolling.

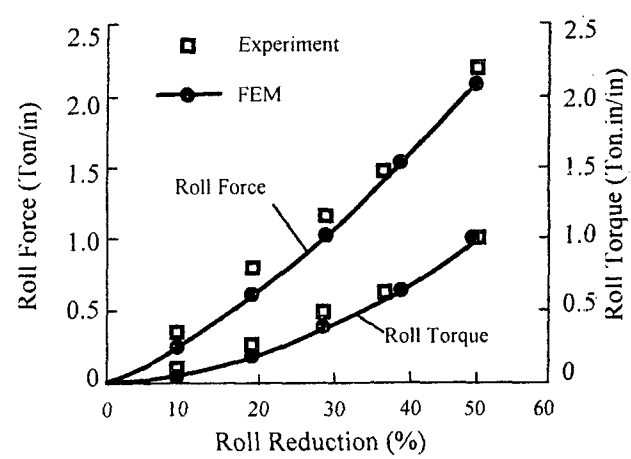

Fig. 11 - Comparative finite element solution and experimental data [12] for sheet metal rolling

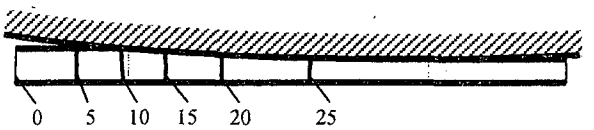

(a) Contact velocity 1 cm/s

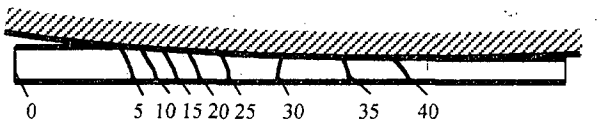

(b) Contact velocity 10 cm/s

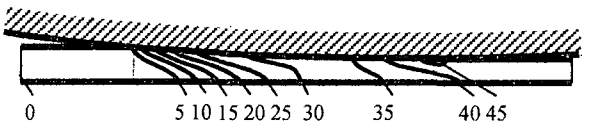

(c) Contact velocity 60 cm/s

Fig. 12 - Predicted temperature distribution in different contact velocities for sheet metal rolling

5. Conclusions

In this paper, the finite element equations were derived and finite element computer program was developed from a set of partial differential equations representing two-dimensional non-Newtonian metal flow. These equations are the conservation of momentums, the conservation of mass and the conservation of energy. The finite element program was used to solve the extrusion and sheet rolling problems. The effects of die area reduction to the extrusion pressure and temperature have been studied. The higher die area reduction produces the higher pressure as well as the higher risen temperature. The velocity solutions at the die corner are improved by the adaptive remeshing technique. The used elements and the computational time are reduced while the solution accuracy is maintained.

Both the extrusion and sheet rolling finite element solutions obtained from the developed finite element program are in good agreement with the analytical solution and the available experimental data. The paper demonstrates the capability of the finite element method that can provide insight to the metal flow behavior under extrusion and sheet rolling.

References

[1] Kobayashi, S., Oh, S. and Altan, T., Metal Forming and The Finite-Element Method, Oxford University press, Oxford, 1989.

[2] Dechaumphai, P., Finite Element for Engineering, Second Ed., Chulalongkorn University Press, Bangkok, 1999.

[3] Peyret, R., Handbook of Computational Fluid Mechnics, Academic press, London, 1996.

[4] Perzyna, P., "Fundamental Problems in Visco-Plasticity," Recent Advances in Applied Mechanics, Academic Press, New York, 1966, Chap. 9, pp. 243-377.

[5] Johnson W. and Melor, P.B., Engineering Plasticity, John Wiley & Sons, New York, 1983.

[6] Yamada, Y., Ito, K., Yokouchi, T. and Ohtsubo, T., "Finite Element Analysis of Steady Fluid and Metal Flow," Finite Element in Fluid, Edited by Gallagher, R.H., et. al., John Wiley and Sons, New York, 1975.

[7] Johnson, W. and Kudo, H., The Mechanics of Metal Extrusion, Manchester University Press, Manchester, 1962.

[8] Johnson, W., "Experiments in Plane-Strain Extrusion," *Journal of the Mechanics of Solids*, Vol. 4, 1956, pp. 269-282.

[9] Dechaumphai, P., "Adaptive Finite Element Technique for Thermal Stress Analysis of Buit-up Structures," *JSME International Journal*, Vol. 39, No. 2, 1996.

[10] Alexander, J.M., "On the Theory of Rolling," *Proc.R.Soc.Lond.A.*, Vol. 326 , 1972, pp. 535-563.

[11] Ford, H. and Alexander, J.M., "Simplified Hot-Rolling Calculations," *Journal of the Institute of Metals*, Vol. 92, 1964, pp. 397-404.

[12] Sims, R.B., "The Calculation of Roll Force and Torque in Hot Rolling Mills," *Proceedings of the Institution of Mechanical Engineers*, Vol. 168, 1954, pp. 191-200.